California Margin temperatures modulate extreme summer precipitation in the desert Southwest

Tripti Bhattacharya,[1*] Ran Feng,[2] Chris R. Maupin,[3] Sloan Coats [4]
Peter R. Brennan,[1], Elizabeth Carter[5]

[1]Department of Earth and Environmental Sciences, Syracuse University, Syracuse NY USA
[2]Department of Geosciences, University of Connecticut, Storrs CT
[3]Department of Geography, Texas A&M University, College Station, TX, USA
[4]Department of Earth Sciences, University of Hawai'i at Manoa, Honolulu, HI, USA
[5]Civil and Environmental Engineering, Syracuse University, Syracuse, NY USA

[*]To whom correspondence should be addressed; E-mail: trbhatta@syr.edu.

This paper is a non-peer reviewed preprint submitted to EarthArXiv.It will be updated as the manuscript progresses through peer review.

California Margin temperatures modulate extreme summer precipitation in the desert Southwest

Tripti Bhattacharya[1*]**,Ran Feng**[2]**, Christopher R. Maupin**[3]**, Sloan Coats**[4]**, Peter R. Brennan**[1]**, Elizabeth Carter**[5]

[1*]Department of Earth and Environmental Sciences, Syracuse University, Syracuse NY USA
[2]Department of Geosciences, University of Connecticut, Storrs, CT, USA
[3]Department of Geography, Texas A&M University, College Station, TX, USA
[4]Department of Earth Sciences, University of Hawai'i at Manoa, Honolulu, HI, USA
[5]Civil and Environmental Engineering, Syracuse University, Syracuse, NY USA
[*] Corresponding Author

E-mail: `trbhatta@syr.edu`

April 2023

Abstract. In August 2022, Death Valley, the driest place in North America, experienced record flooding from summertime rainfall associated with the North American Monsoon (NAM). Given the socioeconomic cost of these type of events, there is a dire need to understand their drivers and future statistics. Fundamental theory predicts that increases in the intensity of precipitation is a robust response to anthropogenic warming. Paleoclimatic evidence suggests that northeast Pacific sea surface temperature (SST) variability could further intensify summertime NAM rainfall over the desert southwest. Drawing on this paleoclimatic evidence, we use historical observations and reanlyses to test the hypothesis that warm SSTs on the southern California margin are linked to more frequent extreme precipitation events in the NAM domain. We find that summers with above-average coastal SSTs are more favorable to moist convection in the northern edge of the NAM domain (southern California, Arizona, New Mexico, and the southern Great Basin). This is because warmer SSTs result in increased precipitable water over normally dry regions of the southwest, driving more frequent precipitation extremes and increases in seasonal rainfall totals. These results, which are robust across observational products, establish a linkage between marine and terrestrial extremes, since summers with anomalously warm SSTs on the California margin have been linked to seasonal or multi-year northeast Pacific marine heatwaves. However, current generation climate models struggle to reproduce the observed relationship between coastal SSTs and NAM precipitation. Across models, there is a strong negative relationship between the magnitude of a models' warm SST bias on the California margin and its skill at reproducing the correlation to desert southwest rainfall. Given persistent northeast Pacific SST biases in models, our results suggest that efforts to improve representation of climatological SSTs are crucial for accurately predicting future changes in hydroclimate extremes in the desert southwest.

Keywords: North American Monsoon, extreme rainfall, southwest hydroclimate

1. Introduction

In August 2022, regions of the desert southwest, including Death Valley, the driest place in North America, experienced once-in-a thousand year flooding. This was a result of summertime storms that dumped up to 75% of normal annual precipitation amounts in the span of a few hours [1]. These storms occurred at the northern edge of the North American Monsoon (NAM), the primary source of summer rainfall in southwestern North America [2, 3]. These types of events are associated with loss of life and infrastructure damage. In addition, above-average monsoon rainfall has been linked to increases in invasive plant biomass, increasing fire risk [4]. These impacts highlight the need to understand the mechanisms underlying variability in regional precipitation extremes.

An increase in precipitation intensity is expected as a result of global warming, since saturation specific humidity increases with temperature [5]. In the NAM region, earth system models (ESMs) and regional models all suggest that warming tends to intensify individual storms, despite predictions of an overall decrease in summer rainfall by the end of the 21st century (albeit with considerable structural uncertainty–[6, 7, 8, 9, 10]). Nevertheless, the entire summer of 2022 featured above-average rainfall, especially on the northern edge of the NAM domain (Figure S1,a). Not only were rainfall rates above average in Nevada, Arizona, and New Mexico, but values of daily outgoing longwave radiation (OLR) show a systematic shift to a longer left tail, suggesting a greater frequency of cooler, convective cloud tops, and associated convective rainfall.

We hypothesize that north Pacific SST variability helped drive these higher rainfall rates. The summer of 2022 featured positive SST anomalies in coastal regions of the northeast Pacific (NEP), as well as a La Niña event in the eastern equatorial Pacific (EEP). Observational analyses have shown that La Niña events feature a stronger monsoon ridge, enhancing the strength of the circulation [11]. Previous analyses of intraseasonal variability in the monsoon found that cool conditions in the EEP cold tongue could drive an earlier monsoon onset [11, 12]. Modeling results, however, are equivocal about the impact of extratropical Pacific SST anomalies on the monsoon. Some studies suggest that warm NEP SST anomalies, similar to the configuration observed in summer 2022, should weaken the monsoon [11]. In contrast, more recent work suggests that these SST anomalies should strengthen the monsoon [13, 14]. Observations and paleoclimatic reconstructions are also equivocal about the relationship between southwest summer precipitation and large-scale SST patterns [15, 16, 17]. Given these contradictory findings, more work is needed to contextualize the role of SST variability in driving extremes similar to summer 2022. Along these lines, paleoclimatic evidence from past warm intervals has identified a link between warm SSTs off the southern California margin and an intensification of monsoon rainfall [18, 13]. If this relationship holds in the modern, it suggests that warm NEP SSTs, as were observed in summer 2022, would have played a role in August 2022 flooding.

In this study, we explore the link between SST on the CA margin and precipitation in the NAM domain. Because of our interest in events similar to the Death Valley flooding in August 2022, we focus on the northern edge of the NAM domain, or regions of the desert southwest in Arizona, New Mexico, California and Nevada. Using observational data, reanalyses, and ESM simulations, we analyze the relationship between large-scale SST patterns and both extreme precipitation and seasonal precipitation totals. We show that summers of a greater frequency of days with extreme precipitation in the northern NAM region tend to co-occur with intervals of warm SSTs on the CA margin. There is also a statistically significant relationship between CA margin SSTs and seasonally-averaged summertime rainfall in the northern NAM domain. Our results therefore provide important context for the processes underlying recent extreme precipitation in the desert southwest, and also identify a mechanism of inter-annual variability in extremes that may continue to influence regional precipitation into the 21st century. However, the ability of Coupled Model Intercomparison Project (CMIP) phase 5 and 6 ESMs to reproduce this relationship is highly variable, and depends in part on the magnitude of SST bias on the CA margin. This has implications for our ability to use ESMs to estimate future changes in extreme precipitation, signal-to-noise ratios, and hydroclimate-related risks in the desert southwest.

2. Data and Methods

2.1. Composite Analyses and Conditional Probability

Our work focuses on the northern NAM region, consisting of land regions of the desert southwest between 28 to 37 °N and 115 to 108 °W. To identify the relationship between daily precipitation extremes and large-scale SST patterns, we used daily Global Precipitation Climatology Centre's (GPCC) 1.0°data to define the 95th percentile of daily precipitation rates at each grid point. This threshold, otherwise known as 'p95', is a widely accepted metric of extreme precipitation for daily average precipitation rates [19]. We then calculated the number of days between June 14th and the end of September in each year that exceed p95 for the interval between 1982 and 2014 [20]. While extreme rainfall is relatively rare in this desert setting, events like August 2022 highlight the profound impact of these types of events. To contextualize extreme precipitation, we analyzed daily fields of outgoing longwave radiation, as an indicator of convective cloud cover and therefore convective rainfall, from NOAA [21]; zonal and meridional moisture flux; and daily maximum 3-hourly convectively available potential energy (CAPE, a measure of energetic favorability of the atmosphere for deep convection and rainfall) from the North American Regional Reanalysis (NARR–[22]). In order to link changes in the frequency of daily precipitation extremes to SST, we analyzed anomalies of monthly SST [23] and total precipitable water [22] associated with summers that contain the greatest frequency of extreme precipitation.

To elucidate the link between CA margin SST anomalies and changes in extreme precipitation in the northern NAM region, we quantified differences in the statistics of Gulf of California surges during summers when an index of CA margin SSTs, averaged between 20 and 30 °N and 125 and 110 °W, is $> 1\sigma$ above average. Gulf surges are daily-scale northward propagation of moisture along the Gulf of California that drive increases in precipitation and humidity in the northern NAM region [24, 25, 26, 27]. Extreme precipitation in the northern

NAM domain tends to be associated with Gulf surges, although not all surges drive high rainfall rates [27]. We used the method outlined in [24] to define gulf surge days (see SI Methods).

Finally, we quantified the probability of seeing a summer with above-average days (e.g., greater than 6 days) with extreme precipitation in the northern NAM region in years with $> 1\sigma$ CA margin SST anomalies. This is essentially the conditional probability that a summer will have greater than 6 days of precipitation exceeding p95 given anomalously warm SSTs on the CA margin. We also assessed this probability for warm CA margin SST anomalies at different lead times (e.g., the preceding April-June SSTs), to see whether preceding CA margin SSTs can serve as predictors of northern NAM region precipitation extremes. The statistical significance of these conditional probabilities was calculated using a 1-sided binomial test to assess whether it was significantly different from random chance (i.e., that the observed conditional probability is not significantly larger than expected from a process with a 50% probability of occurrence [28]).

2.2. Correlation Analysis and Comparison with ESM Simulations

We quantified the correlation between CA margin SSTs and monthly mean precipitation over the northern NAM domain by correlating the same index of CA margin SSTs (20 and 30 °N and 125 and 110 °W) with monthly mean precipitation from multiple precipitation products (0.25 °GPCC product between 1960 and 2014, the CPC merged analysis of precipitation (CPC), the Global Precipitation Climatology Project (GPCP), and the NARR [20, 29, 30, 22]). Using multiple precipitation products helps establish the robustness of the relationship. We also analyzed the correlation between the CA margin SST index and monthly mean fields of precipitable water from the NARR, and sea level pressure from the NCEP-NCAR reanalysis [31]. This complements our analysis of precipitation extremes by showing how CA margin SSTs modulate desert southwest hydroclimate on monthly to seasonal timescales. It also facilitates comparison to CMIP ESMs, since daily-scale fields are unavailable for many models.

To determine the extent to which CMIP5 and CMIP6 ESMs reproduce the observed relationship between CA margin SSTs, precipitation, and circulation, we analyzed historical simulations (Table S1). We analyze historical simulations from 23 ESMs in total, including several conducted as part of the HighResMIP project [32, 33, 34]. Because the set of simulations we analyze differ in their input forcing datasets (e.g., CMIP5 vs. CMIP6 historical simulations), we focused on analyzing the sensitivity of precipitation to CA margin SSTs instead of analyzing the particular trajectory of NAM precipitation in each simulation. We quantified the linear correlation between southern CA Margin SSTs (e.g., the previously defined SST index between 22 and 30 °N and 125 and 110 °W) and northern NAM region precipitation (e.g., the region between 28 to 37 °N and 115 to 108 °W).

3. Results and Discussion

3.1. California margin temperatures and northern NAM region precipitation

Between 1979 and 2014, five summers featured the greatest number of days with rainfall exceeding p95 [19, 35] (Figure 1a). The composite SST pattern associated with these five summers reveals a 'horseshoe' pattern of warmth in the NEP similar to the warm phase of Pacific decadal variability and the extratropical expression of warm ENSO events [36] (Figure 1e), with stronger anomalies near Alaska and off the CA margin. The extratropical portion of this SST pattern resembles that found in summer 2022 (Figure S1d). However, unlike 2022, the EEP cold tongue shows only weakly positive SST anomalies, reflecting that these five years featured different phases of ENSO. While some years featured La Niña events (e.g., 1984, 1990, 1996), others had moderate or decaying El Niño events (e.g. 1983, 2014). The lack of a consistent ENSO phase associated with years of more frequent extreme daily precipitation likely reflects the relatively weak relationship between ENSO and NAM precipitation [11]. It also suggests that NEP SST patterns may play a more important role in modulating the NAM than the EEP, although we note that tropical and extratropical variability are connected [36].

Warmer CA margin SSTs appear to modulate precipitation by driving stronger evaporation and thus increasing precipitable water over the southwest. The five years with the highest number of days exceeding p95 feature higher precipitable water over Baja California, southern California and Arizona, and the Great Basin, representing an almost 50% increase in humidity in some of these regions (Figure 1b,S2). Higher humidity would increase dewpoint temperatures over the normally dry desert regions of the southwest. The 5 years also show a statistically significant shift to larger values of daily maximum 3-hourly CAPE, indicating an increase in the energetic potential of the atmosphere to generate deep convection (Figure 1d) [37]. Similarly, the distribution of daily outgoing longwave radiation during the five years has a larger left tail, reflecting days with deeper convection (Figure 1c), and more convective rainfall.

In years with warm (e.g., $> 1\sigma$) CA margin SST anomalies, there tends to be a higher number of days classified as gulf surges, although this difference is not statistically significant (Figure 2c). There is also no significant shift in the strength of winds associated with gulf surges in years where CA margin SSTs are anomalously warm. However, meridional moisture transport during days with gulf surges is significantly higher in years with anomalously warm CA margin SSTs, bolstering our argument that they influence hydroclimate by modulating humidity (Figure 2d). The increased moisture means that a given daily-scale transient (e.g., a gulf surge) carries more moisture into the NAM region. In the climatology, relatively cool SSTs on the CA margin favor the import of low-entropy air over the northern NAM region [37]. The additional evaporation and humidity from positive CA margin SST anomalies drive higher daily-scale moisture influxes into the northern NAM region, resulting in more CAPE and overall higher summertime precipitation rates [37, 38].

These results suggest that warm SSTs on the CA margin promote an energetic environment that is more favorable for summertime convective storms in the northern NAM domain, resulting in a greater number of days with extreme precipitation. It is notable that at least two of the five years used in this analysis coincide with significant seasonally-persistent extratropical marine heat waves (e.g. 1990, 2014) [39], suggesting a link between marine and atmospheric extremes. The link between total precipitable water off the southern California coast and extreme NAM precipitation has been noted in studies of individual flood events [40, 41], but the link to coastal SSTs has not been explicitly studied. Our results therefore complement and corroborate previous findings using regional modeling (e.g., WRF), which found a linkage between the warm phase of the Pacific Decadal Oscillation (PDO), integrated vapor transport, and an enhanced monsoon [14].

3.2. Implications for Seasonal Prediction

While CA margin SSTs can exhibit significant sub-seasonal SST variability [42], they tend to show strong persistence on monthly to seasonal timescales, with significant correlation between early spring and summertime SST anomalies (Figure S4). This inherent persistence, and the link between CA margin SSTs and northern NAM precipitation extremes, raises the possibility that that coastal SSTs in springtime could aid with efforts to predict northern NAM precipitation.

To test this possibility, we quantified the conditional probability of a summer containing an above-average number of days exceeding p95 given that CA margin SSTs are anomalously warm (e.g., greater than 1σ above average) for different seasonal leads. When CA margin SSTs are 1σ above average in JAS, there is a 85% probability of seeing greater than average days with precipitation exceeding p95 (Figure 2). Warm CA margin SST anomalies during early summer (JJA, MJJ) and spring (AMJ) are also associated with summers with above-average days with precipitation exceeding p95. Each of these relationships are statistically significant at the 95% level (1-sided binomial test [28]). These results highlights the potential utility of coastal SSTs for predicting summers with greater extreme precipitation days in the desert southwest.

3.3. Model Representation of SST-Summer Rainfall Relationship

Figures 1 and 2 suggest that summers with anomalously warm CA margin SSTs not only feature more extreme precipitation days, but also see an overall shift to conditions that are favorable to heavier rainfall. Further support for this interpretation comes from the statistically significant correlations between CA Margin SSTs and total summer (JAS) precipitation in the northern NAM, extending from the northern Sierra Madre Occidental to Baja California and into the Great Basin, across multiple precipitation products (Figure 3,S3). SST anomalies are also positively correlated with total precipitable water in the eastern Pacific and Baja California, with correlations extending north over the Great Basin to almost 40 °N. In a reanalysis (e.g. NCEP-NCAR reanalysis, [31]), CA margin SSTs are correlated with a decrease in surface pressure offshore of Mexico and Baja California, and higher pressures over the Gulf of California. Previous work has noted that on daily timescales, a pressure dipole between the eastern Pacific and the Gulf of California may favor the development of gulf surges, especially those associated with the northward passage of an easterly wave [43, 25, 26, 44, 45]. However, on monthly timescales, the negative correlation over the eastern Pacific likely reflects a decrease in static stability as a result of warmer SSTs and increased humidity [46].

Predicting future risks from flooding, drought, and fire therefore requires an understanding of future NAM-related precipitation extremes. Since most future projections of the NAM system rely on downscaled (or direct) output from ESMs, we assess whether ESMs reproduce the relationship between NEP SSTs and summer rainfall similar to that found in observational products (Figure 3).

Only a small subset of ESMs simulate a similar strength of CA margin - northern NAM precipitation correlation as compared to observational products. Furthermore, we find a significant negative correlation between climatological SST bias on the CA margin and the strength of the correlation to northern NAM summer precipitation: ESMs that are too warm in the CA margin relative to observations underestimate the correlation between summer precipitation and SSTs (Figure 4). For two ESMs, increasing resolution results in an improvement in both the CA Margin SST bias and the correlation to NAM summer precipitation (Figure S5-S7). This coheres with previous findings that higher resolution ESMs perform better at simulating the NAM because of their ability to resolve topography and produce realistic statistics of transient disturbances like gulf surges [47, 10, 48]. However, higher resolution does not always improve the correlation: the higher resolution configuration of the CNRM model produces a weaker CA Margin SST-NAM summer precipitation correlation than its low resolution counterpart (Figure 4).

The results in Figure 4 suggest a role for atmosphere-ocean coupling in driving the strength of the CA Margin SST-NAM summer precipitation correlation. We hypothesize that larger CA margin SST biases result in an atmospheric boundary layer that is less sensitive to SST variability. For models with a strong warm bias on the CA margin, a given SST anomaly may result in a smaller fractional change in humidity or surface moist entropy (e.g. equivalent potential temperature) than in a less biased model. ESMs with a stronger warm bias may therefore generate less variability in NAM precipitation, as well as a weaker link between CA margin SST variability and atmospheric stability. An analysis of the spread across ESMs supports this view, since ESMs with a stronger SST bias on the CA Margin exhibit an overall weaker correlation between SST and sea level pressure on the CA Margin in historical simulations(Figure 4c). This suggests that mean state biases in CMIP ESMs directly influences their ability to capture coupling between SST variability, the atmosphere, and regional hydroclimate. While atmosphere-ocean coupling means that atmospheric biases and oceanic biases influence each other, our hypothesis agrees with previous idealized studies showing that SST patterns modulate ESM skill at simulating rainfall patterns [18, 13, 14, 49, 7].

4. Conclusions

In this paper, we used observational data and reanalyses to demonstrate a linkage between subtropical NEP SSTs and precipitation over the US southwest, Baja California, and western Mexico, which comprise the northern edge of the modern NAM domain. Warm SSTs on the CA margin result in greater evaporation and an increase in precipitable water over coastal regions, creating a summertime energetic environment that is on-average more favorable for moist convection. Warmer SSTs therefore result in a statistically significant increase in the number of days with extreme precipitation, as well as an overall increase in summertime precipitation. Because SST anomalies on CA margin show strong monthly to inter-seasonal persistence, spring or early summer SST anomalies could be used to predict years with a greater frequency of daily precipitation extremes, as well as above-average summertime precipitation in this region. Our results suggest that the extreme precipitation observed in August 2022 was at least in part modulated by the large-scale SST configuration, and that other similar events have occurred over the observational record.

The link between SSTs and NAM precipitation has been explored in previous observational and modeling studies, but results have been equivocal [15, 16, 17, 11, 14]. This may stem from the fact that the SST configuration associated with greater daily precipitation extremes does not resemble a canonical warm ENSO or positive PDO phase. Moreover, the strongest SST-rainfall correlations occur in the northern NAM domain and are relatively weak in the core monsoon domain in western Mexico. Studies that focus on mode-based indices like ENSO or the PDO, or analyze precipitation only in the core monsoon domain, may therefore have missed this association between SST anomalies on the CA margin and NAM rainfall. Our observational analyses support results from paleoclimate studies and modeling efforts that emphasize the importance of the extratropical North Pacific, even in the absence of strong equatorial Pacific SST anomalies, in governing the spatial footprint of NAM precipitation [14, 13, 18].

Over the recent observational record, interannual SST variability on the CA margin has been linked to persistent multi-year marine heat waves [10, 50]. While previous work has explored the linkage between marine heat waves and winter precipitation over western North America [51], we provide an observational link between extreme events in the marine realm and extreme *summertime* precipitation on land. Given that observational data and paleoclimate records suggest strong decadal variability of CA margin SSTs, our results also raise the possibility for decadal modulation of precipitation extremes in the desert southwest [52]. While there is some evidence for decadal variability in NAM precipitation extremes, more long-term precipitation datasets, including paleoclimate proxy datasets, are needed to explore this possibility [16, 17].

While we focus on the link between CA margin SST anomalies and NAM rainfall, it is possible that the strength of this relationship is modulated by equatorial Pacific SSTs. El Niño events result in a southward shift of the intertropical convergence zone in the eastern Pacific, enhancing atmospheric stability over the southwest [6]. In addition, central Pacific El Niño events may reduce NAM rainfall by inhibiting the development of disturbances that can serve as precursors to strong gulf surges [53]. We are unable to disentangle the relative influence of subtropical versus tropical SSTs on northern NAM precipitation in this study because of the limited observational record that offers few realizations of extreme precipitation events, especially since tropical and subtropical SST variability are highly correlated. Long ESM simulations, as well as more idealized modeling studies, could help parse out the importance of subtropical versus tropical SST variability on desert southwest precipitation.

Finally, we showed that historical simulations of ESMs show varying skill at reproducing the correlation between CA Margin SSTs and northern NAM precipitation. ESMs featuring a strong warm bias on the CA Margin show a weaker correlation, in some cases producing significant correlations of the wrong sign. This appears to be related to the fact that ESMs with a strong warm bias underestimate the coupling strength of surface pressure and SST on the CA margin. Both CMIP5 and CMIP6 ESMs exhibit systematic warm SST biases in the subtropical NEP, likely stemming from biases in shortwave radiation and ocean heat transport [54, 55]. Given the results presented herein, ESMs are likely to systematically misrepresent an important source of interannual variability in desert southwest precipitation. This in turn undermines confidence in the results of studies that rely on direct or downscaled ESM outputs to quantify future changes in precipitation extremes, estimate signal-to-noise ratios for regional hydroclimate, or analyze future changes in hydroclimate-related risk over the desert southwest [56, 57]. ESMs are also known to underestimate the severity and duration of multi-month or multi-year marine heat waves, similar to those that cause warming on the southern CA margin [58]. Efforts to improve ESM representation of climatological SSTs and SST variability will therefore greatly improve our ability to estimate variability and trends in precipitation extremes, with broad implications for our understanding of future regional hydroclimate, especially in arid regions like the desert southwest.

It remains an open question as to whether the relationship between SSTs on the CA margin and northern NAM precipitation will persist into the 21st century. Modeling studies predict a weakening of the NAM with anthropogenic warming, in part from a dynamic response resulting in a warmer, more stable troposphere over the southwest [6] and thus a higher threshold for convection [7]. This suggests that in the future, a given CA margin SST anomaly may become less effective at generating positive anomalies of CAPE over the northern NAM region, resulting in a decrease in the strength of the correlation to summertime precipitation in this region. We briefly assess this possibility by analyzing the four ESMs that best reproduce the observed CA margin SST-northern NAM precipitation correlation, and find that all produce a strong, statistically significant correlation well into the 21st century, with two ESMs even producing a strengthening of this association (Figure S9). While further analyses, especially using large ensemble approaches, are needed to disentangle the relative influence of interannual SST variability and forced changes on future precipitation in the northern NAM region, our results suggest that the CA margin SST-NAM monsoon linkage could aid the effort to predict monsoon extremes well into the 21st century.

5. Acknowledgments

The authors thank John Chiang (University of California Berkeley) for valuable feedback on this work. TB acknowledges funding from NSF P2C2 Grant OCE-1903148 and OCE-2103015. RF acknowledges funding from NSF P2C2 Grant OCE-1903650 and OCE-2103055.

6. References

[1] Gabriel Canon. Record death valley flooding 'a once-in-1,000-year event'. *The Guardian*, 2022.

[2] Benjamin I Cook and RICHARD Seager. The response of the North American Monsoon to increased greenhouse gas forcing. *Journal of Geophysical Research: Atmospheres*, 118(4):1690–1699, 2013.

[3] David K Adams and Andrew C Comrie. The north american monsoon. *Bulletin of the American Meteorological Society*, 78(10):2197–2214, 1997.

[4] Kirk A Moloney, Erika L Mudrak, Andres Fuentes-Ramirez, Hadas Parag, Marjolein Schat, and Claus Holzapfel. Increased fire risk in Mojave and Sonoran shrublands due to exotic species and extreme rainfall events. *Ecosphere*, 10(2):e02592, 2019.

[5] Paul A. O'Gorman. Precipitation Extremes Under Climate Change. *Current Climate Change Reports*, 1(2):49–59, June 2015.

[6] Salvatore Pascale, William R Boos, Simona Bordoni, Thomas L Delworth, Sarah B Kapnick, Hiroyuki Murakami, Gabriel A Vecchi, and Wei Zhang. Weakening of the North American monsoon with global warming. *Nature Climate Change*, 7(11):806–812, 2017.

[7] Salvatore Pascale, Sarah B Kapnick, Simona Bordoni, and Thomas L Delworth. The influence of CO2 forcing on North American monsoon moisture surges. *Journal of Climate*, 31(19):7949–7968, 2018.

[8] Mansour Almazroui, M Nazrul Islam, Fahad Saeed, Sajjad Saeed, Muhammad Ismail, Muhammad Azhar Ehsan, Ismaila Diallo, Enda O'Brien, Moetasim Ashfaq, Daniel Martínez-Castro, et al. Projected changes in temperature and precipitation over the united states, central america, and the caribbean in cmip6 gcms. *Earth Systems and Environment*, 5:1–24, 2021.

[9] Suyeon Moon and Kyung-Ja Ha. Future changes in monsoon duration and precipitation using CMIP6. *npj Climate and Atmospheric Science*, 3(1):45, 2020.

[10] Jonathan DD Meyer and Jiming Jin. The response of future projections of the North American monsoon when combining dynamical downscaling and bias correction of CCSM4 output. *Climate Dynamics*, 49(1-2):433–447, 2017.

[11] Christopher L Castro, Thomas B McKee, and Roger A Pielke. The relationship of the North American monsoon to tropical and North Pacific sea surface temperatures as revealed by observational analyses. *Journal of Climate*, 14(24):4449–4473, 2001.

[12] Stephen W Bieda, Christopher L Castro, Steven L Mullen, Andrew C Comrie, and Erik Pytlak. The relationship of transient upper-level troughs to variability of the North American monsoon system. *Journal of Climate*, 22(15):4213–4227, 2009.

[13] Fu, Minmin and Cane, Mark A and Molnar, Peter and Tziperman, Eli. Warmer pliocene upwelling site sst leads to wetter subtropical coastal areas: A positive feedback on sst. *Paleoceanography and Paleoclimatology*, 37(2):e2021PA004357, 2022.

[14] É Beaudin, E Di Lorenzo, AJ Miller, H Seo, and Y Joh. Impact of Extratropical Northeast Pacific SST on US West Coast Precipitation. *Geophysical Research Letters*, 50(3):e2022GL102354, 2023.

[15] Carlos M Carrillo, Christopher L Castro, Connie A Woodhouse, and Daniel Griffin. Low-frequency variability of precipitation in the North American monsoon region as diagnosed through earlywood and latewood tree-ring chronologies in the southwestern US. *International Journal of Climatology*, 36(5):2254–2272, 2016.

[16] Eleonora MC Demaria, Pieter Hazenberg, Russell L Scott, Menberu B Meles, Mary Nichols, and David

Goodrich. Intensification of the North American Monsoon rainfall as observed from a long-term high-density gauge network. *Geophysical Research Letters*, 46(12):6839–6847, 2019.

[17] Daniel Griffin, Connie A Woodhouse, David M Meko, David W Stahle, Holly L Faulstich, Carlos Carrillo, Ramzi Touchan, Christopher L Castro, and Steven W Leavitt. North american monsoon precipitation reconstructed from tree-ring latewood. *Geophysical Research Letters*, 40(5):954–958, 2013.

[18] Bhattacharya, Tripti and Feng, Ran and Tierney, Jessica E and Rubbelke, Claire and Burls, Natalie and Knapp, Scott and Fu, Minmin. Expansion and intensification of the north american monsoon during the pliocene. *AGU Advances*, 3(6):e2022AV000757, 2022.

[19] J Sillmann, VV Kharin, X Zhang, FW Zwiers, and D Bronaugh. Climate extremes indices in the CMIP5 multimodel ensemble: Part 1. Model evaluation in the present climate. *Journal of geophysical research: atmospheres*, 118(4):1716–1733, 2013.

[20] Udo Schneider, Tobias Fuchs, Anja Meyer-Christoffer, and Bruno Rudolf. Global precipitation analysis products of the GPCC. *Global Precipitation Climatology Centre (GPCC), DWD, Internet Publikation*, 112, 2008.

[21] Brant Liebmann and Catherine A Smith. Description of a complete (interpolated) outgoing longwave radiation dataset. *Bulletin of the American Meteorological Society*, 77(6):1275–1277, 1996.

[22] Fedor Mesinger, Geoff DiMego, Eugenia Kalnay, Kenneth Mitchell, Perry C Shafran, Wesley Ebisuzaki, Dušan Jović, Jack Woollen, Eric Rogers, Ernesto H Berbery, Michael B Ek, Yun Fan, Robert Grumbine, W Higgins, Hong Li, Ying Lin, Geoff Manikin, David Parrish, and Wei Shi. North American regional reanalysis. *Bulletin of the American Meteorological Society*, 87(3):343–360, 2006.

[23] Masayoshi Ishii, Akiko Shouji, Satoshi Sugimoto, and Takanori Matsumoto. Objective analyses of sea-surface temperature and marine meteorological variables for the 20th century using icoads and the kobe collection. *International Journal of Climatology: A Journal of the Royal Meteorological Society*, 25(7):865–879, 2005.

[24] Salvatore Pascale and Simona Bordoni. Tropical and extratropical controls of Gulf of California surges and summertime precipitation over the southwestern United States. *Monthly Weather Review*, 144(7):2695–2718, 2016.

[25] Simona Bordoni and Bjorn Stevens. Principal component analysis of the summertime winds over the Gulf of California: A gulf surge index. *Monthly weather review*, 134(11):3395–3414, 2006.

[26] David J Stensrud, Robert L Gall, and Mel K Nordquist. Surges over the Gulf of California during the Mexican monsoon. *Monthly Weather Review*, 125(4):417–437, 1997.

[27] RW Higgins and W Shi. Relationships between Gulf of California moisture surges and tropical cyclones in the eastern Pacific basin. *Journal of Climate*, 18(22):4601–4620, 2005.

[28] Daniel S Wilks. *Statistical Methods in the Atmospheric Sciences*, volume 100. Academic press, 2011.

[29] Pingping Xie, Phillip A Arkin, and John E Janowiak. CMAP: The CPC merged analysis of precipitation. *Measuring precipitation from space*, 28:319–328, 2007.

[30] Robert F Adler, Mathew RP Sapiano, George J Huffman, Jian-Jian Wang, Guojun Gu, David Bolvin, Long Chiu, Udo Schneider, Andreas Becker, Eric Nelkin, Pingping Xie, R Ferraro, and Dong-Bin Shin. The global precipitation climatology project (gpcp) monthly analysis (new version 2.3) and a review of 2017 global precipitation. *Atmosphere*, 9(4):138, 2018.

[31] Eugenia Kalnay, Masao Kanamitsu, Robert Kistler, William Collins, Dennis Deaven, Lev Gandin, Mark Iredell, Suranjana Saha, Glenn White, John Woollen, Y. Zhu, M. Ebisuzaki Chelliah, W. Higgins, J. Janowiak, K.C. Mo, C. Ropelewski, J. Wang, A. Leetmaa, R. Reynolds, R. Jenne, and D. Joseph. The NCEP/NCAR 40-year reanalysis project. *Bulletin of the American meteorological Society*, 77(3):437–472, 1996.

[32] Ping Chang, Shaoqing Zhang, Gokhan Danabasoglu, Stephen G Yeager, Haohuan Fu, Hong Wang, Frederic S Castruccio, Yuhu Chen, James Edwards, Dan Fu, et al. An unprecedented set of high-resolution earth system simulations for understanding multiscale interactions in climate variability and change. *Journal of Advances in Modeling Earth Systems*, 12(12):e2020MS002298, 2020.

[33] Reindert J Haarsma, Malcolm J Roberts, Pier Luigi Vidale, Catherine A Senior, Alessio Bellucci, Qing Bao, Ping Chang, Susanna Corti, Neven S Fučkar, Virginie Guemas, et al. High resolution

model intercomparison project (HighResMIP v1. 0) for CMIP6. *Geoscientific Model Development*, 9(11):4185–4208, 2016.

[34] Veronika Eyring, Sandrine Bony, Gerald A Meehl, Catherine A Senior, Bjorn Stevens, Ronald J Stouffer, and Karl E Taylor. Overview of the coupled model intercomparison project phase 6 (cmip6) experimental design and organization. *Geoscientific Model Development*, 9(5):1937–1958, 2016.

[35] Tereza Cavazos, C Turrent, and DP Lettenmaier. Extreme precipitation trends associated with tropical cyclones in the core of the North American monsoon. *Geophysical Research Letters*, 35(21), 2008.

[36] E Di Lorenzo, T Xu, Y Zhao, M Newman, A Capotondi, S Stevenson, DJ Amaya, BT Anderson, R Ding, JC Furtado, et al. Modes and mechanisms of pacific decadal-scale variability. *Annual Review of Marine Science*, 15:249–275, 2023.

[37] Tripti Bhattacharya. An Energetic Perspective on the Holocene North American Monsoon. *Geophysical Research Letters*, 49(19):e2022GL100782, 2022.

[38] Mariam Fonseca-Hernandez, Cuauhtémoc Turrent, Yandy G Mayor, and Iryna Tereshchenko. Using observational and reanalysis data to explore the southern Gulf of California boundary layer during the North American Monsoon onset. *Journal of Geophysical Research: Atmospheres*, 126(7):e2020JD033508, 2021.

[39] A Capotondi, M Newman, T Xu, and E Di Lorenzo. An optimal precursor of Northeast Pacific marine heatwaves and Central Pacific El Niño events. *Geophysical Research Letters*, 49(5):e2021GL097350, 2022.

[40] Long Yang, James Smith, Mary Lynn Baeck, Efrat Morin, and David C Goodrich. Flash flooding in arid/semiarid regions: Dissecting the hydrometeorology and hydrology of the 19 August 2014 storm and flood hydroclimatology in Arizona. *Journal of Hydrometeorology*, 18(12):3103–3123, 2017.

[41] Jeremy J Mazon, Christopher L Castro, David K Adams, Hsin-I Chang, Carlos M Carrillo, and John J Brost. Objective climatological analysis of extreme weather events in Arizona during the North American monsoon. *Journal of Applied Meteorology and Climatology*, 55(11):2431–2450, 2016.

[42] Xinyue Wei, Kai-Yuan Li, Thomas Kilpatrick, Minyang Wang, and Shang-Ping Xie. Large-scale conditions for the record-setting Southern California marine heatwave of August 2018. *Geophysical Research Letters*, 48(7):e2020GL091803, 2021.

[43] David J Raymond, Christopher S Bretherton, and John Molinari. Dynamics of the intertropical convergence zone of the east Pacific. *Journal of the atmospheric sciences*, 63(2):582–597, 2006.

[44] Ryan D Fuller and David J Stensrud. The relationship between tropical easterly waves and surges over the Gulf of California during the North American monsoon. *Monthly weather review*, 128(8):2983–2989, 2000.

[45] RW Higgins, Wei Shi, and Christopher Hain. Relationships between Gulf of California moisture surges and precipitation in the southwestern United States. *Journal of Climate*, 17(15):2983–2997, 2004.

[46] Timothy A Myers, Carlos R Mechoso, Gregory V Cesana, Michael J DeFlorio, and Duane E Waliser. Cloud feedback key to marine heatwave off Baja California. *Geophysical Research Letters*, 45(9):4345–4352, 2018.

[47] Salvatore Pascale, Simona Bordoni, Sarah B Kapnick, Gabriel A Vecchi, Liwei Jia, Thomas L Delworth, Seth Underwood, and Whit Anderson. The impact of horizontal resolution on north american monsoon gulf of california moisture surges in a suite of coupled global climate models. *Journal of Climate*, 29(21):7911–7936, 2016.

[48] Arianna M Varuolo-Clarke, Kevin A Reed, and Brian Medeiros. Characterizing the North American monsoon in the Community Atmosphere Model: Sensitivity to resolution and topography. *Journal of Climate*, 32(23):8355–8372, 2019.

[49] Salvatore Pascale, Leila M. V. Carvalho, David K. Adams, Christopher L. Castro, and Iracema F. A. Cavalcanti. Current and Future Variations of the Monsoons of the Americas in a Warming Climate. *Current Climate Change Reports*, 5(3):125–144, September 2019.

[50] Melanie R Fewings and Kevin S Brown. Regional structure in the marine heat wave of summer 2015 off the western United States. *Frontiers in Marine Science*, 6:564, 2019.

[51] Daniel L Swain, Michael Tsiang, Matz Haugen, Deepti Singh, Allison Charland, Bala Rajaratnam, and

Noah S Diffenbaugh. The extraordinary California drought of 2013/2014: Character, context, and the role of climate change. *Bulletin of the American Meteorological Society*, 95(9):S3, 2014.

[52] Nicholas A. O'Mara, Anson H. Cheung, Christopher S. Kelly, Samantha Sandwick, Timothy D. Herbert, James M. Russell, Jose Abella-Gutiérrez, Sylvia G. Dee, Peter W. Swarzenski, and Juan Carlos Herguera. Subtropical Pacific Ocean Temperature Fluctuations in the Common Era: Multidecadal Variability and Its Relationship With Southwestern North American Megadroughts. *Geophysical Research Letters*, 46(24):14662–14673, December 2019.

[53] Hye-Mi Kim, Peter J Webster, and Judith A Curry. Modulation of North Pacific tropical cyclone activity by three phases of ENSO. *Journal of Climate*, 24(6):1839–1849, 2011.

[54] Qibei Zhang, Bo Liu, Shuanglin Li, and Tianjun Zhou. Understanding Models' Global Sea Surface Temperature Bias in Mean State: From CMIP5 to CMIP6. *Geophysical Research Letters*, 50(4), February 2023.

[55] Robert CJ Wills, Yue Dong, Cristian Proistosecu, Kyle C Armour, and David S Battisti. Systematic Climate Model Biases in the Large-Scale Patterns of Recent Sea-Surface Temperature and Sea-Level Pressure Change. *Geophysical Research Letters*, 49(17):e2022GL100011, 2022.

[56] Amir AghaKouchak, Felicia Chiang, Laurie S. Huning, Charlotte A. Love, Iman Mallakpour, Omid Mazdiyasni, Hamed Moftakhari, Simon Michael Papalexiou, Elisa Ragno, and Mojtaba Sadegh. Climate Extremes and Compound Hazards in a Warming World. *Annual Review of Earth and Planetary Sciences*, 48(1):519–548, May 2020.

[57] Kate Marvel, Benjamin I Cook, Céline JW Bonfils, Paul J Durack, Jason E Smerdon, and A Park Williams. Twentieth-century hydroclimate changes consistent with human influence. *Nature*, 569(7754):59–65, 2019.

[58] Sandra M Plecha and Pedro MM Soares. Global marine heatwave events using the new cmip6 multi-model ensemble: from shortcomings in present climate to future projections. *Environmental Research Letters*, 15(12):124058, 2020.

7. Figures and Figure Captions

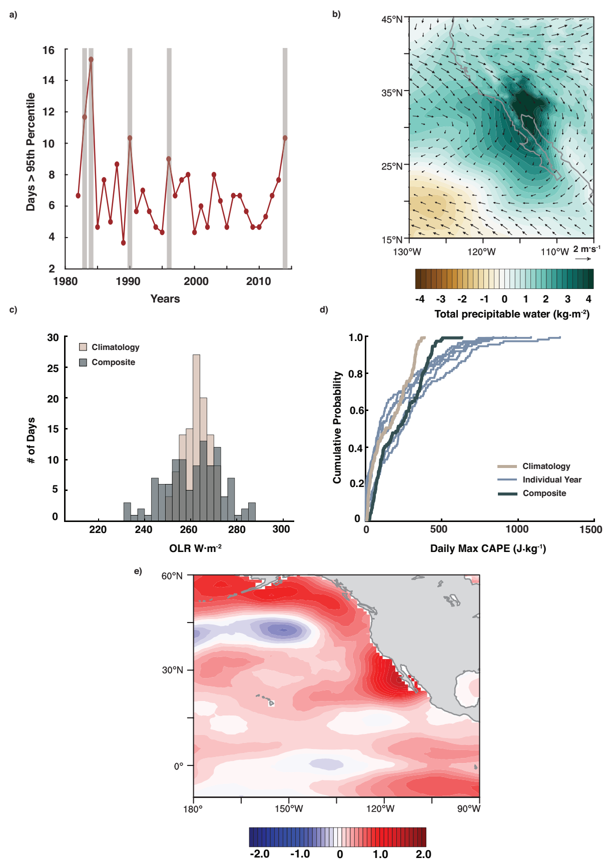

Figure 1. Composites associated with summers featuring the greatest number of extreme precipitation days a) shows the number of summertime days with precipitation exceeding the 95th percentile (p95) between 1981 and 2014 over the region between 28 and 37 °N and 115 and 108 °W. Gray bars highlight the five years with the greatest number of extreme precipitation days (1983, 1984, 1990, 1996, and 2014). b) total precipitable water during these five summers. c) outgoing longwave radiation (OLR) associated with these five summers (green) compared to climatology (tan). d) shows daily maximum of 3-hourly CAPE for climatology (tan), each individual summer (light blue) and a composite of all summers (dark blue). In both panels c) and d), composites are significantly different at the 95% level from the climatological distribution (2-sample Kolmogorov-Smirnov test). d) shows the SST composite associated with these five summers.

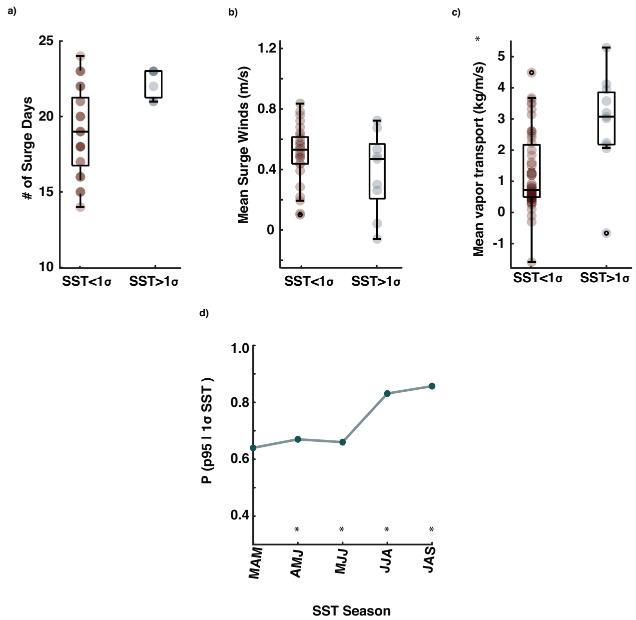

Figure 2. Changes in the average statistics of Gulf of California surges with and without anomalously warm CA margin SSTs. a) differences in the number of days classified as gulf surges in years where CA margin SST anomalies are less than 1σ above average (red), compared to the number of gulf surge days in summers where CA margin SST anomalies are above 1σ (blue). b) as in a) but for average wind speeds over the northern Gulf of California (25 to 32°N and 115 to 105°W) on days classified as gulf surges; c) as in a) but for meridional moisture flux over the northern Gulf of California during gulf surge days; this shift is statistically significant at the 95% level using a 1-sided 2-sample Kolmogorov-Smirnov test. d) probability of seeing greater than 6 days of precipitation above p95 between July and September in the presence of a warm SST anomaly on the CA margin at different leading seasons. Seasons with $*$ are statistically significant at the 95% level using a 1-sided binomial test.

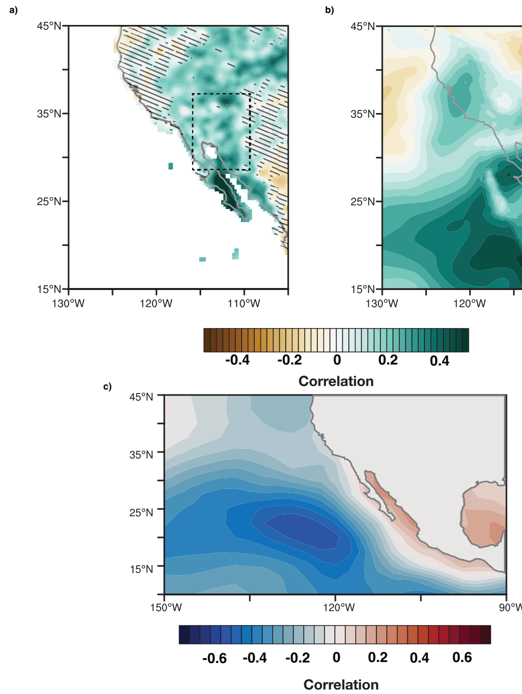

Figure 3. Correlation between CA margin SSTs and southwest hydroclimate. a) Shows the linear correlation between the CA margin SST index and summer July-September precipitation, with hatching indicating regions where correlations are not statistically significant at the 95% level. b) correlation between summertime CA margin SSTs and total precipitable water. c) correlation between summertime CA margin SSTs and and sea level pressure.

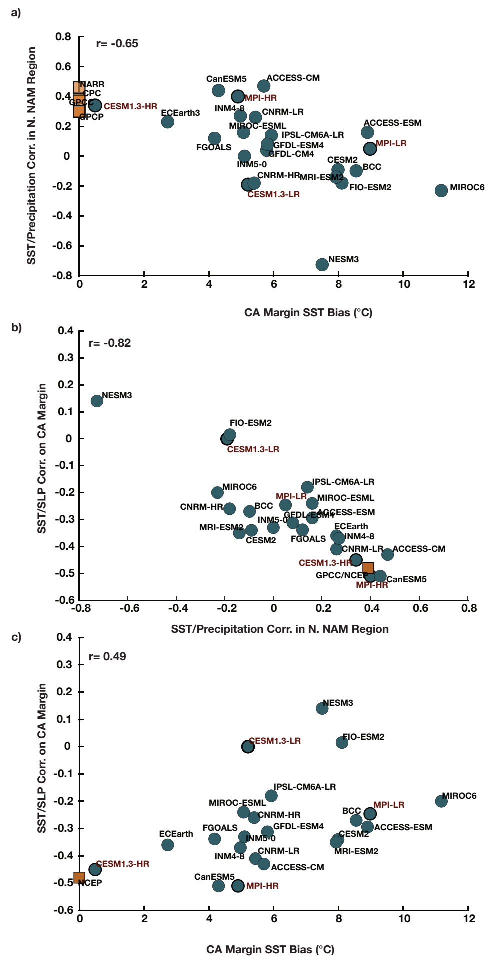

Figure 4. Relationship between SST bias and hydroclimate in observational products compared to CMIP5 and CMIP6 ESMs. a) Scatterplot of SST bias over 20 and 30 °N and 125 and 110 °W on the CA margin (x axis), and the strength of the correlation between SSTs in this region and precipitation in the northern NAM region (27 and 37 °N and 115 and 107 °W–y axis). b) Relationship between the strength of precipitation-SST correlation shown in panel a (x axis) and the correlation between SLP (20 and 30 °N and 125 and 110 °W) and SST over CA margin (y axis); c) Relationship between SST bias on the CA margin (x axis) and the SLP-SST correlation shown in panel b (y axis).

Supplemental Information for *California Margin temperatures modulate extreme summer precipitation in the desert Southwest*

Tripti Bhattacharya[1], Ran Feng[2], Christopher R. Maupin[3], Sloan Coats[4], Elizabeth Carter[5], and Peter R. Brennan[1]

[1]Department of Earth and Environmental Sciences, Syracuse University, Syracuse, NY, USA

[2]Department of Geosciences, University of Connecticut, Storrs, CT, USA

[3]Department of Geography, Texas A&M University, College Station, TX, USA

[4]Department of Earth Sciences, University of Hawai'i at Manoa, Honolulu, HI, USA

[5]Civil and Environmental Engineering, Syracuse University, Syracuse, NY USA

May 31, 2023

Contents of this file

Text S1. Additional Methods Description

Gulf Surge Analysis

We analyzed changes in Gulf of California surges during summers with above-average (e.g., 1σ above the mean) sea surface temperature (SST) on the southern California margin (CA margin). Gulf of California surges refer to daily-scale transients that transport moisture along the Gulf of California, driving increases in humidity and high rainfall rates over the desert southwest *Pascale and Bordoni* (2016); *Bordoni and Stevens* (2006); *Stensrud et al.* (1997); *Higgins and Shi* (2005). Strong gulf surges, especially those associated with the passage of a tropical easterly wave to the south of the Gulf of California, tend to be associated with extreme precipitation over Arizona and other parts of the northern edge of the North American Monsoon (NAM) domain *Pascale and Bordoni* (2016). However, gulf surges can be 'dry' and not associated with high rainfall rates *Higgins and Shi* (2005). We therefore chose to quantify whether there are a greater number of Gulf surges in years with CA margin warming, as well as whether those surge days are associated with stronger mean daily winds or stronger mean daily moisture transport over the northern Gulf of California. For these latter two metrics, we take averages of winds and daily meridional moisture transport over 25 to 32°N and 115 to 105°W.

We used the method outlined in *Pascale and Bordoni* (2016) to define gulf surge days. This method uses the first two EOFs of near-surface along-shore winds, obtained after removing the daily-scale seasonal cycle from the wind field, over the entire Gulf of California to classify surge days and non-surge days. We performed this analysis using data from the North American Regional Reanalysis (NARR), but obtain similar EOFs with similar amounts of variance explained to those in *Pascale and Bordoni* (2016). Given the relatively short observational record, this analysis should be seen as largely exploratory, since we only have a few years in our observational record that feature summers of CA margin SSTs that are 1σ or more above the mean. Longer term datasets, or long integrations of high-resolution Earth System Model (ESM) simulations, may be essential to demonstrate the link between the statistics of gulf surges and SST variability.

Correlation and Running Correlation Analysis

To identify the link between CA margin SSTs and monthly mean precipitation over the northern NAM domain, we calculated an index of SSTs between 20 and 30 °N and 125 and 110 °W. We then calculated the linear correlation of this index and monthly mean precipitation fields from the 0.25 °Global Precipitation Climatology Centre (GPCC) product between 1960 and 2014, the Climate Prediction Center merged analysis of precipitation (CPC), the Global Precipitation Climatology Project (GPCP), and the NARR *Schneider et al.* (2008); *Xie et al.* (2007); *Adler et al.* (2018); *Mesinger et al.* (2006). Using multiple precipitation products helps establish the robustness of the relationship. We also evaluated the correlation between this SST index and monthly mean fields of SLP, precipitable water, and moisture flux from the NARR.

For our analysis of correlations between CA margin SSTs and precipitation across a range of Coupled Model Intercomparison Project (CMIP) phase 5 and 6 ESMs, we use an index of precipitation over land areas between 27 and 37 °N and 115 and 107 °W. For the SST-sea level pressure (SLP) correlation analysis, we use an index of SLP over ocean areas between 20 and 30 °N and 125 and 110 °W. Slight changes to the bounds of these index regions do not alter our results or conclusions.

In Figure **S9**, we plot the running correlation between CA margin SST anomalies and precipitation in future emission scenarios for the 4 ESMs that show the greatest fidelity over the historical period at producing the observed SST-precipitation correlation (high resolution configurations of CESM1.3, MPI-ESM1-2, as well as ACCESS-CM and CanESM5). This running correlation is performed in 40-year averaging windows for historical simulations, Shared Socioeconomic Pathway (SSP) 3-7.0 and 5-8.5 in the case of the MPI, ACCESS and CanESM5 ESMs, and for Representative Concentration Pathway (RCP) 8.5 in the case of CESM1.3-HR (see Table S1 for more details). Because the forcing datasets differ across these simulations, the purpose of this analysis is not to analyze the particular trajectory of NAM precipitation and SST in a given ESM versus another, although we show this in Figure **S8**. Instead, the goal of this analysis is show that the strength of the correlation between CA margin SSTs and northern NAM precipitation remains statistically significant in the future.

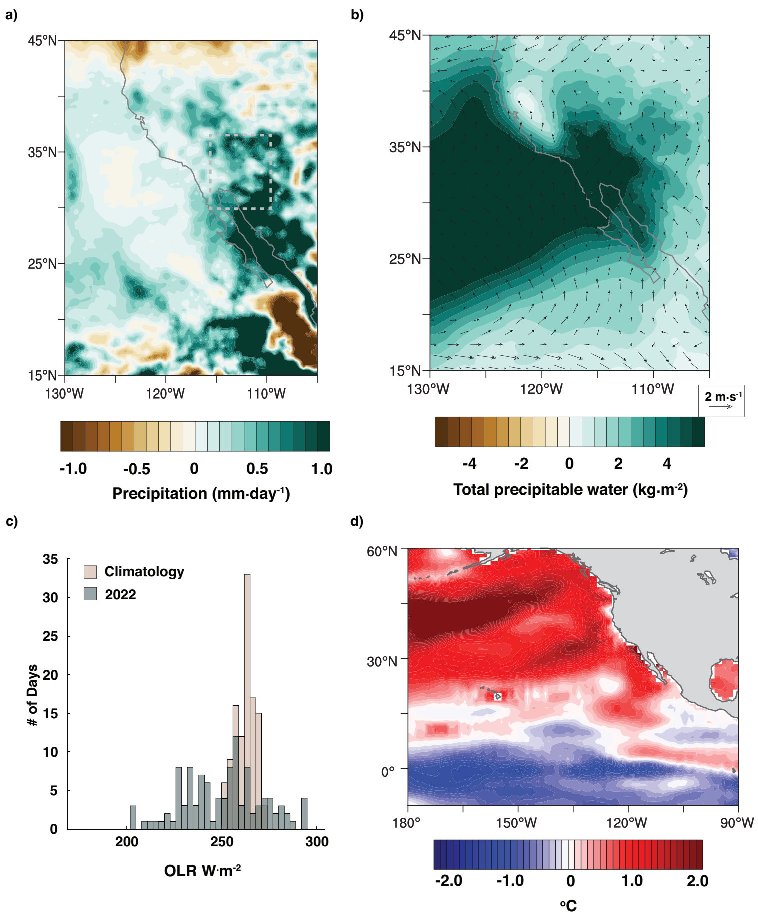

Figure S1: **Shifts in monsoon precipitation rates in summer 2022.** a) shows July-September monthly mean precipitation anomalies in mm/day. Gray box highlights the northern NAM region used for averaging, and includes Death Valley, CA. b) shows anomalies of total precipitable water and 850 mb winds. c) shows differences in daily values of outgoing longwave radiation (OLR) for summer 2022 (mint green) compared to the climatology between 1974 and 2022 (tan). The distribution of OLR for 2022 is significantly different from the climatological distribution at the 95% level according to a 2-sided Kolmogorov-Smirnov (K-S) test. d) shows summer 2022 SST anomalies in °C relative to a 1950-2022 climatology.

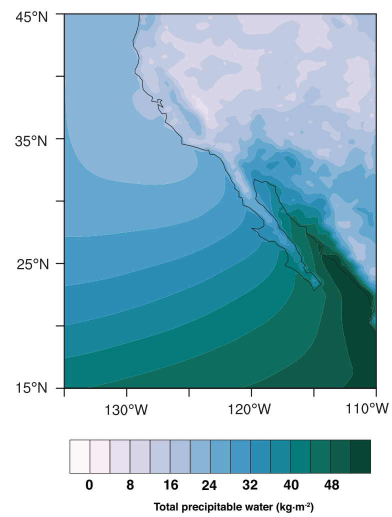

Figure S2: July-September climatology of total precipitable water in kg/m^2 over the southwest US and western Mexico. Data from the North American Regional Reanalysis (*Mesinger et al.*, 2006). Climatology shows strong gradients from 30-40 °N, where there are very low values of precipitable water over desert regions of the southwest.

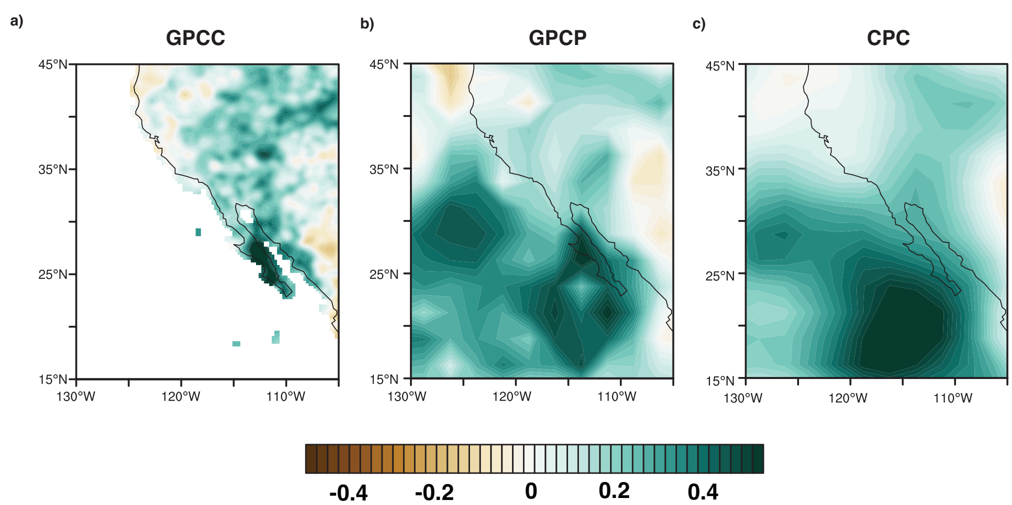

Figure S3: Correlation between CA Margin SSTs and southwestern precipitation between July-September across three different precipitation products. SSTs are an index between 22 and 30 °N and 125 and 110 °W, taken from the COBE SST product (*Ishii et al.*, 2005). a) shows GPCC correlation from the main text (*Schneider et al.*, 2008); b) shows correlation with GPCP (*Adler et al.*, 2018); and c) shows correlation between SSTs and CPC precipitation (*Xie et al.*, 2007). Results show that the correlation pattern is robust across observational products.

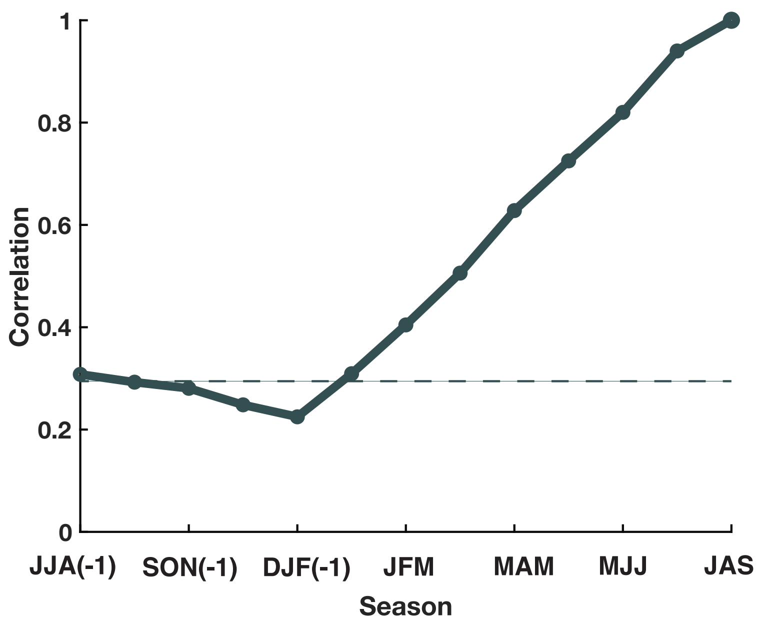

Figure S4: Correlation between July-September (JAS) SST anomalies on the CA Margin (20 and 30 °N and 125 and 110 °W) and simultaneous (JAS) and prior seasons' SST anomalies, starting with JJA, then MJJ, AMJ, MAM, etc. until JJA in the prior year. Significance of correlation level is indicated by the dashed line.

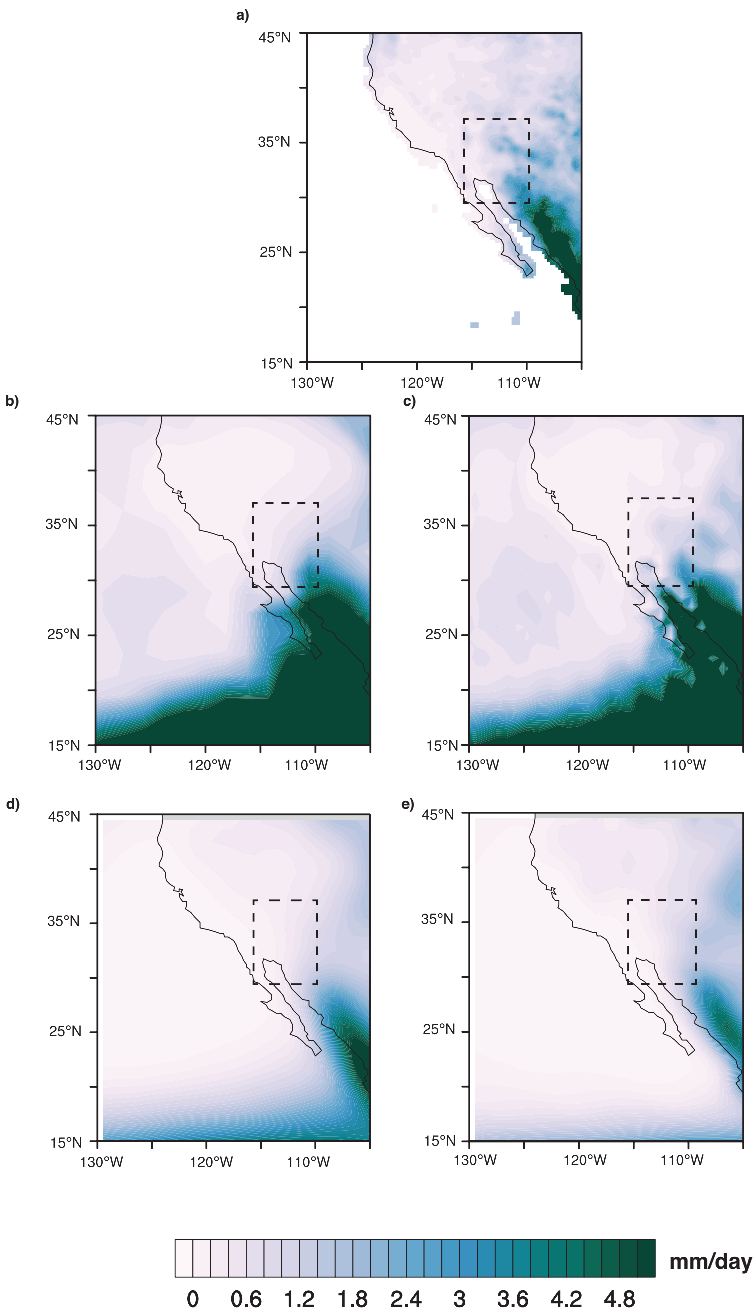

Figure S5: July-September climatology of low vs. high resolution ESMs. a) shows observational climatology of summertime precipitation from the GPCC 0.25 °product; b) shows MPI-ESM1-2 low resolution summertime rainfall climatology; c) shows MPI-ESM1-2 high resolution climatology; d) shows CESM1.3 low resolution climatology; e) shows CESM1.3 high resolution climatology. All ESM climatologies are computed from 1950-2014 in historical simulations. Dashed box outlines the region used for precipitation averages shown in Figure 5 in the main text. Climatologies of rainfall rates show a small improvement over this dashed box in the high resolution version of the ESMs

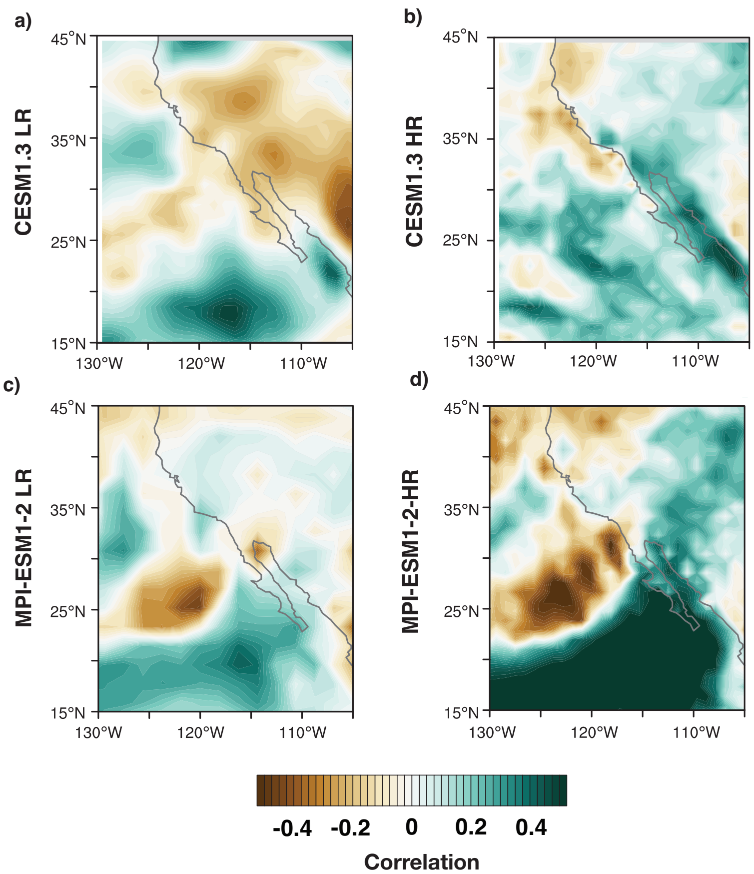

Figure S6: July-September correlation of precipitation with CA margin SST anomalies in historical simulations to analyze impact of changing resolution. a) CESM1.3 low resolution; b) CESM1.3 high resolution; c) MPI-ESM1-2 low resolution; d) MPI-ESM1-2 high resolution. In the higher resolution simulations, positive correlations with SST extend farther north into the Great Basin.

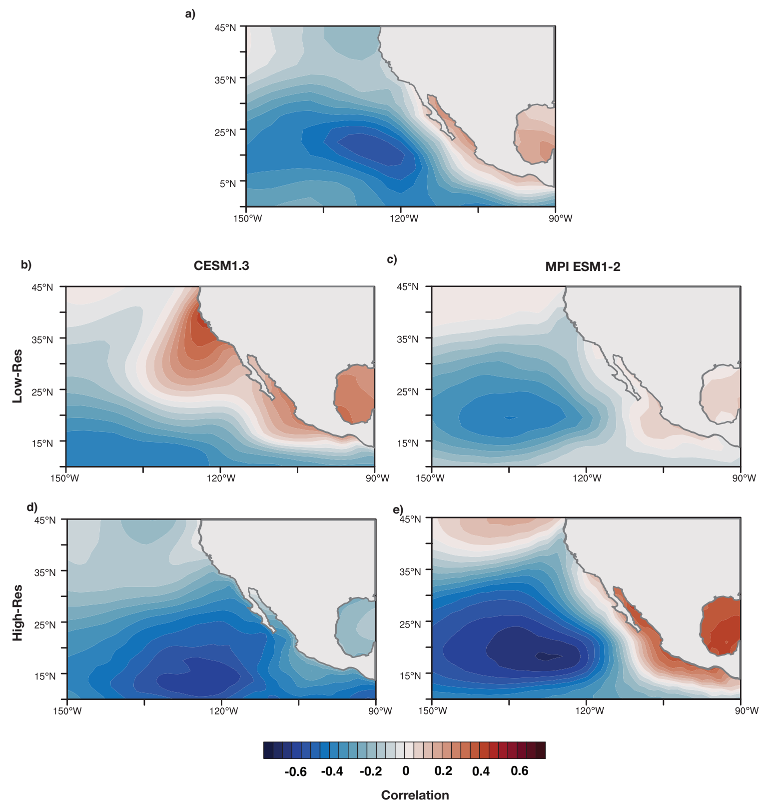

Figure S7: July-September correlation of SLP with CA margin SST anomalies in historical simulations to analyze impact of changing resolution. a) CESM1.3 low resolution; b) CESM1.3 high resolution; c) MPI-ESM1-2 low resolution; d) MPI-ESM1-2 high resolution. Higher resolution simulations, which also have a smaller SST bias on the CA margin, produce a stronger correlation between SLP and CA margin SSTs.

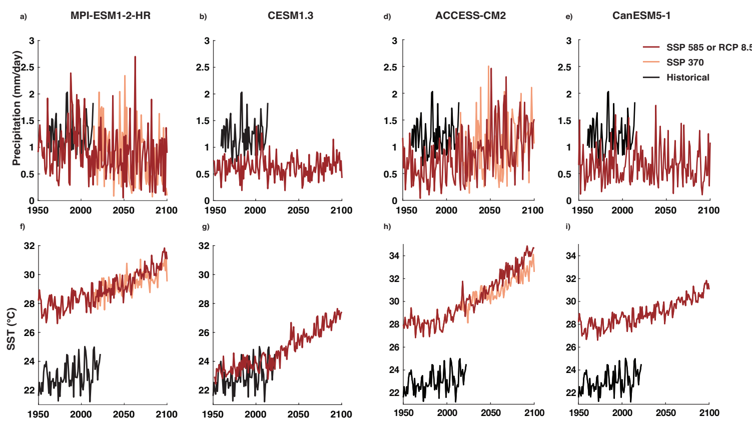

Figure S8: Changes in precipitation and SST in the future for ESMs that exhibit CA margin SST-northern NAM rainfall correlations similar to observations. Top panel shows precipitation (mm/day); bottom panel shows SST (°C). a) and f) are MPI-ESM1-2; b) and g) are CESM1.3; c) and h) are ACCESS-CM2; and d) and i) are CanESM5-1. SSTs and precipitation are in absolute units rather than anomalies in order to highlight SST and precipitation biases.

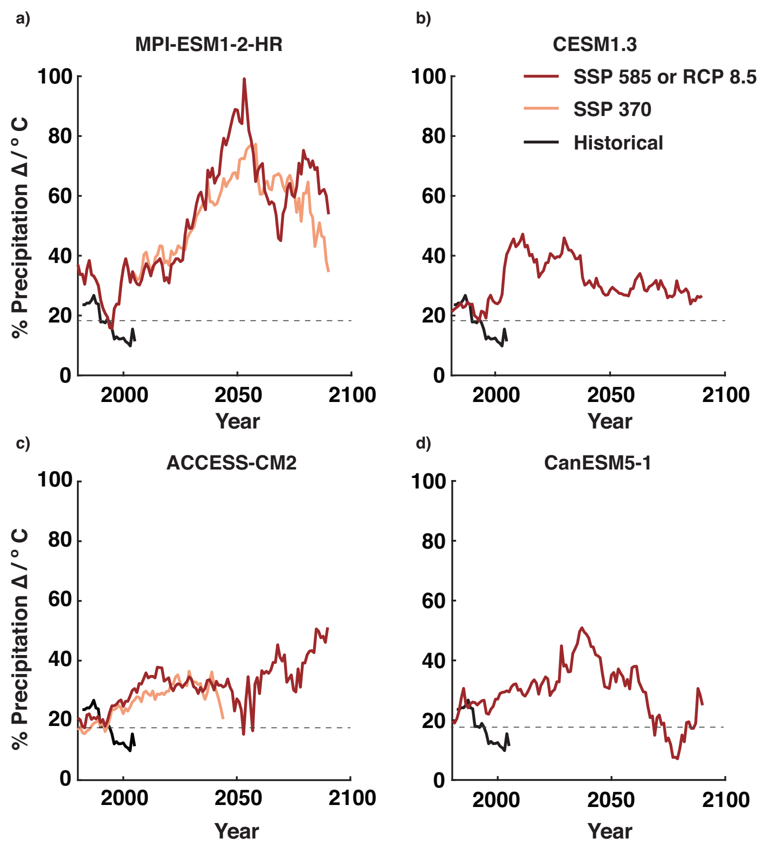

Figure S9: Running correlation between CA margin SST and precipitation for future emissions scenarios across four ESMs that show the highest skill at reproducing the observed SST-precipitation correlation (see Figure 4 in main text). Correlations above the dashed line are statistically significant at the 95% level.

Table S1: CMIP6 and CMIP5 models used to analyze the relationship between SST bias between 22 and 30 °N and 125 and 110 °W, on the CA margin, and the relationship between SSTs, precipitation, and SLP over northern NAM domain shown in Figure 4 and Figure 5 in the main text. Acronym refers to the acronym used in Figure 4 in the main text.

Institution	Model Name	Acronym	Simulations Analyzed
National Center for Atmospheric Research	CESM2	CESM2	CMIP6 historical
National Center for Atmospheric Research	CESM1.3 low-res	CESM1.3 LR	CMIP5 historical
National Center for Atmospheric Research	CESM1.3 high-res	CESM1.3 HR	CMIP5 historical RCP8.5
EC Earth Consortium	EC-Earth3	ECEarth3	CMIP6 historical
Model for Interdisciplinary Research on Climate	MIROC6	MIROC6	CMIP6 historical
Model for Interdisciplinary Research on Climate	MIROC-ESM2-L	MIROC-ESML	CMIP6 historical
Geophysical Fluid Dynamics Laboratory	GFDL-CM4	GFDL-CM4	CMIP6 historical
Geophysical Fluid Dynamics Laboratory	GFDL-ESM4	GFDL-ESM4	CMIP6 historical
L'Institut Pierre-Simon Laplace	IPSL-CM6A-LR	IPSL-CM6A-LR	CMIP6 historical
Beijing Climate Center	BCC-CSM2-MR	BCC	CMIP6 historical
State Key Laboratory of Numerical Modeling for Atmospheric Sciences and Geophysical Fluid Dynamics	FGOALS-g3	FGOALS	CMIP6 historical
Max Planck Institute for Meteorology	MPI-ESM1-2-LR	MPI-LR	CMIP6 historical
Max Planck Institute for Meteorology	MPI-ESM1-2-HR	MPI-HR	CMIP6 historical SSP585 SSP370
Canadian Centre for Climate Modelling and Analysis	CanESM5-1	CanESM5	CMIP6 historical SSP585
Centre National de Recherches Météorologiques	CNRM-CM6-1	CNRM-LR	CMIP6 historical
Centre National de Recherches Météorologiques	CNRM-CM6-1	CNRM-HR	CMIP6 historical
Commonwealth Scientific & Industrial Research Organisation Australia	ACCESS-CM2	ACCESS-CM	CMIP6 historical SSP585 SSP370
Commonwealth Scientific and Industrial Research Organisation Australia	ACCESS-ESM2	ACCESS-ESM	CMIP6 historical
Nanjing University of Information Science and Technology China	NESM3	NESM3	CMIP6 historical
First Institute of Oceanography and Pilot National Laboratory for Marine Science and Technology	FIO-ESM2	IO-ESM2	CMIP6 historical
Meteorological Research Institute Japan	MRI-ESM-2.0	MRI-ESM2	CMIP6 historical
Institute for Numerical Mathematics Russian Federation	INM-CM4-8	INM4-8	CMIP6 historical
Institute for Numerical Mathematics Russian Federation	INM-CM5-0	INM5-0	CMIP6 historical

References

Adams, D. K., and A. C. Comrie (1997), The north american monsoon, *Bulletin of the American Meteorological Society*, *78*(10), 2197–2214.

Adams, J. L., and D. J. Stensrud (2007), Impact of tropical easterly waves on the North American monsoon, *Journal of climate*, *20*(7), 1219–1238.

Adler, R. F., M. R. Sapiano, G. J. Huffman, J.-J. Wang, G. Gu, D. Bolvin, L. Chiu, U. Schneider, A. Becker, E. Nelkin, P. Xie, R. Ferraro, and D.-B. Shin (2018), The global precipitation climatology project (gpcp) monthly analysis (new version 2.3) and a review of 2017 global precipitation, *Atmosphere*, *9*(4), 138.

AghaKouchak, A., F. Chiang, L. S. Huning, C. A. Love, I. Mallakpour, O. Mazdiyasni, H. Moftakhari, S. M. Papalexiou, E. Ragno, and M. Sadegh (2020), Climate Extremes and Compound Hazards in a Warming World, *Annual Review of Earth and Planetary Sciences*, *48*(1), 519–548, doi:10.1146/annurev-earth-071719-055228.

Almazroui, M., M. N. Islam, F. Saeed, S. Saeed, M. Ismail, M. A. Ehsan, I. Diallo, E. O'Brien, M. Ashfaq, D. Martínez-Castro, et al. (2021), Projected changes in temperature and precipitation over the united states, central america, and the caribbean in cmip6 gcms, *Earth Systems and Environment*, *5*, 1–24.

Beaudin, É., E. Di Lorenzo, A. Miller, H. Seo, and Y. Joh (2023), Impact of Extratropical Northeast Pacific SST on US West Coast Precipitation, *Geophysical Research Letters*, *50*(3), e2022GL102,354.

Bhattacharya, T. (2022), An Energetic Perspective on the Holocene North American Monsoon, *Geophysical Research Letters*, *49*(19), e2022GL100,782.

Bhattacharya, Tripti and Feng, Ran and Tierney, Jessica E and Rubbelke, Claire and Burls, Natalie and Knapp, Scott and Fu, Minmin (2022), Expansion and intensification of the north american monsoon during the pliocene, *AGU Advances*, *3*(6), e2022AV000,757.

Bieda, S. W., C. L. Castro, S. L. Mullen, A. C. Comrie, and E. Pytlak (2009), The relationship of transient upper-level troughs to variability of the North American monsoon system, *Journal of Climate*, *22*(15), 4213–4227.

Bordoni, S., and B. Stevens (2006), Principal component analysis of the summertime winds over the Gulf of California: A gulf surge index, *Monthly weather review*, *134*(11), 3395–3414.

Canon, G. (2022), Record death valley flooding 'a once-in-1,000-year event', *The Guardian*.

Capotondi, A., M. Newman, T. Xu, and E. Di Lorenzo (2022), An optimal precursor of Northeast Pacific marine heatwaves and Central Pacific El Niño events, *Geophysical Research Letters*, *49*(5), e2021GL097,350.

Carrillo, C. M., C. L. Castro, C. A. Woodhouse, and D. Griffin (2016), Low-frequency variability of precipitation in the North American monsoon region as diagnosed through earlywood and latewood tree-ring chronologies in the southwestern US, *International Journal of Climatology*, *36*(5), 2254–2272.

Castro, C. L., T. B. McKee, and R. A. Pielke (2001), The relationship of the North American monsoon to tropical and North Pacific sea surface temperatures as revealed by observational analyses, *Journal of Climate*, *14*(24), 4449–4473.

Castro, C. L., R. A. Pielke, J. O. Adegoke, S. D. Schubert, and P. J. Pegion (2007), Investigation of the summer climate of the contiguous United States and Mexico using the Regional Atmospheric Modeling System (RAMS). Part II: Model climate variability, *Journal of Climate*, *20*(15), 3866–3887.

Cavazos, T., C. Turrent, and D. Lettenmaier (2008), Extreme precipitation trends associated with tropical cyclones in the core of the North American monsoon, *Geophysical Research Letters*, *35*(21).

Chang, P., S. Zhang, G. Danabasoglu, S. G. Yeager, H. Fu, H. Wang, F. S. Castruccio, Y. Chen, J. Edwards, D. Fu, et al. (2020), An unprecedented set of high-resolution earth system simulations for understanding multiscale interactions in climate variability and change, *Journal of Advances in Modeling Earth Systems*, *12*(12), e2020MS002,298.

Cook, B. I., and R. Seager (2013), The response of the North American Monsoon to increased greenhouse gas forcing, *Journal of Geophysical Research: Atmospheres*, *118*(4), 1690–1699.

Demaria, E. M., P. Hazenberg, R. L. Scott, M. B. Meles, M. Nichols, and D. Goodrich (2019), Intensification of the North American Monsoon rainfall as observed from a long-term high-density gauge network, *Geophysical Research Letters*, *46*(12), 6839–6847.

Di Lorenzo, E., T. Xu, Y. Zhao, M. Newman, A. Capotondi, S. Stevenson, D. Amaya, B. Anderson, R. Ding, J. Furtado, et al. (2023), Modes and mechanisms of pacific decadal-scale variability, *Annual Review of Marine Science*, *15*, 249–275.

Eyring, V., S. Bony, G. A. Meehl, C. A. Senior, B. Stevens, R. J. Stouffer, and K. E. Taylor (2016), Overview of the coupled model intercomparison project phase 6 (cmip6) experimental design and organization, *Geoscientific Model Development*, *9*(5), 1937–1958.

Fewings, M. R., and K. S. Brown (2019), Regional structure in the marine heat wave of summer 2015 off the western United States, *Frontiers in Marine Science*, *6*, 564.

Fonseca-Hernandez, M., C. Turrent, Y. G. Mayor, and I. Tereshchenko (2021), Using observational and reanalysis data to explore the southern Gulf of California boundary layer during the North American Monsoon onset, *Journal of Geophysical Research: Atmospheres*, *126*(7), e2020JD033,508.

Fu, Minmin and Cane, Mark A and Molnar, Peter and Tziperman, Eli (2022), Warmer pliocene upwelling site sst leads to wetter subtropical coastal areas: A positive feedback on sst, *Paleoceanography and Paleoclimatology*, *37*(2), e2021PA004,357.

Fuller, R. D., and D. J. Stensrud (2000), The relationship between tropical easterly waves and surges over the Gulf of California during the North American monsoon, *Monthly weather review*, *128*(8), 2983–2989.

Griffin, D., C. A. Woodhouse, D. M. Meko, D. W. Stahle, H. L. Faulstich, C. Carrillo, R. Touchan, C. L. Castro, and S. W. Leavitt (2013), North american monsoon precipitation reconstructed from tree-ring latewood, *Geophysical Research Letters*, *40*(5), 954–958.

Haarsma, R. J., M. J. Roberts, P. L. Vidale, C. A. Senior, A. Bellucci, Q. Bao, P. Chang, S. Corti, N. S. Fučkar, V. Guemas, et al. (2016), High resolution model intercomparison project (HighResMIP v1. 0) for CMIP6, *Geoscientific Model Development*, *9*(11), 4185–4208.

Higgins, R., and W. Shi (2005), Relationships between Gulf of California moisture surges and tropical cyclones in the eastern Pacific basin, *Journal of Climate*, *18*(22), 4601–4620.

Higgins, R., W. Shi, and C. Hain (2004), Relationships between Gulf of California moisture surges and precipitation in the southwestern United States, *Journal of Climate*, *17*(15), 2983–2997.

Huang, B., V. F. Banzon, E. Freeman, J. Lawrimore, W. Liu, T. C. Peterson, T. M. Smith, P. W. Thorne, S. D. Woodruff, and H.-M. Zhang (2015), Extended reconstructed sea surface temperature version 4 (ersst. v4). part i: Upgrades and intercomparisons, *Journal of climate*, *28*(3), 911–930.

Ishii, M., A. Shouji, S. Sugimoto, and T. Matsumoto (2005), Objective analyses of sea-surface temperature and marine meteorological variables for the 20th century using icoads and the kobe collection, *International Journal of Climatology: A Journal of the Royal Meteorological Society*, *25*(7), 865–879.

Kalnay, E., M. Kanamitsu, R. Kistler, W. Collins, D. Deaven, L. Gandin, M. Iredell, S. Saha, G. White, J. Woollen, Y. Zhu, M. E. Chelliah, W. Higgins, J. Janowiak, K. Mo, C. Ropelewski, J. Wang, A. Leetmaa, R. Reynolds, R. Jenne, and D. Joseph (1996), The NCEP/NCAR 40-year reanalysis project, *Bulletin of the American meteorological Society*, *77*(3), 437–472.

Kim, H.-M., P. J. Webster, and J. A. Curry (2011), Modulation of North Pacific tropical cyclone activity by three phases of ENSO, *Journal of Climate*, *24*(6), 1839–1849.

Liebmann, B., and C. A. Smith (1996), Description of a complete (interpolated) outgoing longwave radiation dataset, *Bulletin of the American Meteorological Society*, *77*(6), 1275–1277.

Marvel, K., B. I. Cook, C. J. Bonfils, P. J. Durack, J. E. Smerdon, and A. P. Williams (2019), Twentieth-century hydroclimate changes consistent with human influence, *Nature*, *569*(7754), 59–65.

Mauritsen, T., J. Bader, T. Becker, J. Behrens, M. Bittner, R. Brokopf, V. Brovkin, M. Claussen, T. Crueger, M. Esch, I. Fast, S. Fiedler, D. Fläschner, V. Gayler, M. Giorgetta, D. S. Goll, H. Haak, S. Hagemann, C. Hedemann, C. Hohenegger, T. Ilyina, T. Jahns, D. Jimenéz-de-la-Cuesta, J. Jungclaus, T. Kleinen, S. Kloster, D. Kracher, S. Kinne, D. Kleberg, G. Lasslop, L. Kornblueh, J. Marotzke, D. Matei, K. Meraner, U. Mikolajewicz, K. Modali, B. Möbis, W. A. Müller, J. E. M. S. Nabel, C. C. W. Nam, D. Notz, S. Nyawira, H. Paulsen, K. Peters, R. Pincus, H. Pohlmann, J. Pongratz, M. Popp, T. J. Raddatz, S. Rast, R. Redler, C. H. Reick, T. Rohrschneider, V. Schemann, H. Schmidt, R. Schnur, U. Schulzweida, K. D. Six, L. Stein, I. Stemmler, B. Stevens, J. Storch, F. Tian, A. Voigt, P. Vrese, K. Wieners, S. Wilkenskjeld, A. Winkler, and E. Roeckner (2019), Developments in the MPI-M Earth System Model version 1.2 (MPI-ESM1.2) and Its Response to Increasing CO_2, *Journal of Advances in Modeling Earth Systems*, *11*(4), 998–1038, doi:10.1029/2018MS001400.

Mazon, J. J., C. L. Castro, D. K. Adams, H.-I. Chang, C. M. Carrillo, and J. J. Brost (2016), Objective climatological analysis of extreme weather events in Arizona during the North American monsoon, *Journal of Applied Meteorology and Climatology*, *55*(11), 2431–2450.

Mesinger, F., G. DiMego, E. Kalnay, K. Mitchell, P. C. Shafran, W. Ebisuzaki, D. Jović, J. Woollen, E. Rogers, E. H. Berbery, M. B. Ek, Y. Fan, R. Grumbine, W. Higgins, H. Li, Y. Lin, G. Manikin, D. Parrish, and W. Shi (2006), North American regional reanalysis, *Bulletin of the American Meteorological Society*, *87*(3), 343–360.

Meyer, J. D., and J. Jin (2017), The response of future projections of the North American monsoon when combining dynamical downscaling and bias correction of CCSM4 output, *Climate Dynamics*, *49*(1-2), 433–447.

Moloney, K. A., E. L. Mudrak, A. Fuentes-Ramirez, H. Parag, M. Schat, and C. Holzapfel (2019), Increased fire risk in Mojave and Sonoran shrublands due to exotic species and extreme rainfall events, *Ecosphere*, *10*(2), e02,592.

Moon, S., and K.-J. Ha (2020), Future changes in monsoon duration and precipitation using CMIP6, *npj Climate and Atmospheric Science*, *3*(1), 45.

Myers, T. A., C. R. Mechoso, G. V. Cesana, M. J. DeFlorio, and D. E. Waliser (2018), Cloud feedback key to marine heatwave off Baja California, *Geophysical Research Letters*, *45*(9), 4345–4352.

Müller, W. A., J. H. Jungclaus, T. Mauritsen, J. Baehr, M. Bittner, R. Budich, F. Bunzel, M. Esch, R. Ghosh, H. Haak, T. Ilyina, T. Kleine, L. Kornblueh, H. Li, K. Modali, D. Notz, H. Pohlmann, E. Roeckner, I. Stemmler, F. Tian, and J. Marotzke (2018), A Higher-resolution Version of the Max Planck Institute Earth System Model (MPI-ESM1.2-HR), *Journal of Advances in Modeling Earth Systems*, *10*(7), 1383–1413, doi:10.1029/2017MS001217.

O'Mara, N. A., A. H. Cheung, C. S. Kelly, S. Sandwick, T. D. Herbert, J. M. Russell, J. Abella-Gutiérrez, S. G. Dee, P. W. Swarzenski, and J. C. Herguera (2019), Subtropical Pacific Ocean Temperature Fluctuations in the Common Era: Multidecadal Variability and Its Relationship With Southwestern North American Megadroughts, *Geophysical Research Letters*, *46*(24), 14,662–14,673, doi:10.1029/2019GL084828.

O'Gorman, P. A. (2015), Precipitation Extremes Under Climate Change, *Current Climate Change Reports*, *1*(2), 49–59, doi:10.1007/s40641-015-0009-3.

Pascale, S., and S. Bordoni (2016), Tropical and extratropical controls of Gulf of California surges and summertime precipitation over the southwestern United States, *Monthly Weather Review*, *144*(7), 2695–2718.

Pascale, S., S. Bordoni, S. B. Kapnick, G. A. Vecchi, L. Jia, T. L. Delworth, S. Underwood, and W. Anderson (2016), The impact of horizontal resolution on north american monsoon gulf of california moisture surges in a suite of coupled global climate models, *Journal of Climate*, *29*(21), 7911–7936.

Pascale, S., W. R. Boos, S. Bordoni, T. L. Delworth, S. B. Kapnick, H. Murakami, G. A. Vecchi, and W. Zhang (2017), Weakening of the North American monsoon with global warming, *Nature Climate Change*, *7*(11), 806–812.

Pascale, S., S. B. Kapnick, S. Bordoni, and T. L. Delworth (2018), The influence of CO2 forcing on North American monsoon moisture surges, *Journal of Climate*, *31*(19), 7949–7968.

Pascale, S., L. M. V. Carvalho, D. K. Adams, C. L. Castro, and I. F. A. Cavalcanti (2019), Current and Future Variations of the Monsoons of the Americas in a Warming Climate, *Current Climate Change Reports*, *5*(3), 125–144, doi:10.1007/s40641-019-00135-w.

Plecha, S. M., and P. M. Soares (2020), Global marine heatwave events using the new CMIP6 multi-model ensemble: from shortcomings in present climate to future projections, *Environmental Research Letters*, *15*(12), 124,058.

Raymond, D. J., C. S. Bretherton, and J. Molinari (2006), Dynamics of the intertropical convergence zone of the east Pacific, *Journal of the atmospheric sciences*, *63*(2), 582–597.

Schneider, U., T. Fuchs, A. Meyer-Christoffer, and B. Rudolf (2008), Global precipitation analysis products of the GPCC, *Global Precipitation Climatology Centre (GPCC), DWD, Internet Publikation*, *112*.

Sillmann, J., V. Kharin, X. Zhang, F. Zwiers, and D. Bronaugh (2013), Climate extremes indices in the CMIP5 multimodel ensemble: Part 1. Model evaluation in the present climate, *Journal of geophysical research: atmospheres*, *118*(4), 1716–1733.

Stensrud, D. J., R. L. Gall, and M. K. Nordquist (1997), Surges over the Gulf of California during the Mexican monsoon, *Monthly Weather Review*, *125*(4), 417–437.

Swain, D. L., M. Tsiang, M. Haugen, D. Singh, A. Charland, B. Rajaratnam, and N. S. Diffenbaugh (2014), The extraordinary California drought of 2013/2014: Character, context, and the role of climate change, *Bulletin of the American Meteorological Society*, *95*(9), S3.

Varuolo-Clarke, A. M., K. A. Reed, and B. Medeiros (2019), Characterizing the North American monsoon in the Community Atmosphere Model: Sensitivity to resolution and topography, *Journal of Climate*, *32*(23), 8355–8372.

Wei, X., K.-Y. Li, T. Kilpatrick, M. Wang, and S.-P. Xie (2021), Large-scale conditions for the record-setting Southern California marine heatwave of August 2018, *Geophysical Research Letters*, *48*(7), e2020GL091,803.

Wilks, D. S. (2011), *Statistical Methods in the Atmospheric Sciences*, vol. 100, Academic press.

Wills, R. C., Y. Dong, C. Proistosecu, K. C. Armour, and D. S. Battisti (2022), Systematic Climate Model Biases in the Large-Scale Patterns of Recent Sea-Surface Temperature and Sea-Level Pressure Change, *Geophysical Research Letters*, *49*(17), e2022GL100,011.

Xie, P., P. A. Arkin, and J. E. Janowiak (2007), CMAP: The CPC merged analysis of precipitation, *Measuring precipitation from space*, *28*, 319–328.

Yang, L., J. Smith, M. L. Baeck, E. Morin, and D. C. Goodrich (2017), Flash flooding in arid/semiarid regions: Dissecting the hydrometeorology and hydrology of the 19 August 2014 storm and flood hydroclimatology in Arizona, *Journal of Hydrometeorology*, *18*(12), 3103–3123.

Zhang, Q., B. Liu, S. Li, and T. Zhou (2023), Understanding Models' Global Sea Surface Temperature Bias in Mean State: From CMIP5 to CMIP6, *Geophysical Research Letters*, *50*(4), doi:10.1029/2022GL100888.